Organic & Biomolecular Chemistry

Accepted Manuscript

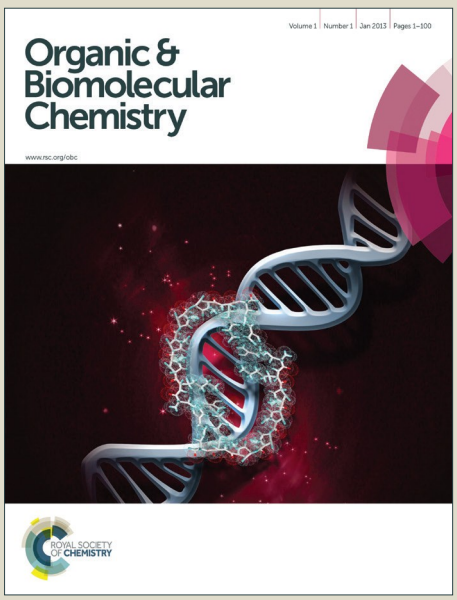

This is an *Accepted Manuscript*, which has been through the Royal Society of Chemistry peer review process and has been accepted for publication.

Accepted Manuscripts are published online shortly after acceptance, before technical editing, formatting and proof reading. Using this free service, authors can make their results available to the community, in citable form, before we publish the edited article. We will replace this *Accepted Manuscript* with the edited and formatted *Advance Article* as soon as it is available.

You can find more information about *Accepted Manuscripts* in the Information for Authors.

Please note that technical editing may introduce minor changes to the text and/or graphics, which may alter content. The journal's standard Terms & Conditions and the Ethical guidelines still apply. In no event shall the Royal Society of Chemistry be held responsible for any errors or omissions in this *Accepted Manuscript* or any consequences arising from the use of any information it contains.

ROYAL SOCIETY OF CHEMISTRY

www.rsc.org/obc

Journal Name

RSCPublishing

ARTICLE

Blue 'turn-on' fluorescent probes for the direct detection of free radicals and nitric oxide in *Pseudomonas aeruginosa* biofilms

Cite this: DOI: 10.1039/x0xx00000x

Received 00th January 2012,
Accepted 00th January 2012

DOI: 10.1039/x0xx00000x

www.rsc.org/

Mina Barzegar Amiri Olia[a,b] Athanasios Zavras,[a,b] Carl H. Schiesser,[*a,b] and Stefanie-Ann Alexander[a,b]

Two novel cell-permeable and bacteria-compatible 'turn-on' fluorescent probes, designed to be compatible in a multi-dye system and to fluoresce in the blue region exhibiting emission maxima of 440-490 nm, were synthesized. The profluorescent nitroxide probe (**11**) was developed to visualize and quantify free radical and redox processes, and the Cu(II)-complexed coumarin-based probe (**16a**) was developed for NO detection. Confocal laser-scanning microscopy and subsequent digital analysis of *Pseudomonas aeruginosa* biofilms stained with **11** or **16a** determined that free radical and redox processes and NO generation occur predominantly in live cells during normal biofilm growth.

Introduction

Surface-associated communities of bacteria, known as biofilms, represent great obstacles in many industries including medicine, shipping and cultural material conservation.[1] These sessile microorganisms are protected within an exopolymeric matrix (EPM) of biomolecules that often render attempts at eradicating problematic biofilms futile.[2] The dispersal of single-celled planktonic bacteria from biofilms is an important mechanism by which the cycle of colonization and infection continues.[3] Although more motile in the planktonic form, bacteria dispersing from the protective embrace of a biofilm become more susceptible to exogenous pressures such as antibiotics and biocides. As such, much research has focused on the development of anti-biofilm agents that effectively disperse biofilms and prevent their formation with the anticipation that they will increase eradication efficacy when used in combination with bactericidal agents.[4]

Knowing precisely how biofilm formation and dispersal are mediated is critical but these mechanisms remain incompletely characterized. The activity of one key dispersal-regulating molecule, nitric oxide (NO), is thought to be attributed to c-di-GMP signalling and has been linked to the accumulation of oxidative stress within *Pseudomonas aeruginosa* microcolonies.[5] That is, hollow vacuoles within the microcolony are created by localized bursts of reactive oxygen (ROS) and nitrogen species (RNS) releasing and dispersing planktonic bacteria from the biofilm structure.[5] The use of NO, in the form of NO-donor compounds, as anti-biofilm agents has been well documented.[6] Furthermore, we have recently identified a novel nitroxide that displays NO-like anti-biofilm activity in *P. aeruginosa* and mixed culture biofilms.[7]

[a]*ARC Centre of Excellence for Free Radical Chemistry and Biotechnology, Australia.*
[b]*School of Chemistry and Bio21 Molecular Science and Biotechnology Institute, The University of Melbourne, Victoria, 3010, Australia. Fax: +61 3 9347 8189; Tel: +61 3 8344 2432; E-mail: carlhs@unimelb.edu.au*

†Electronic Supplementary Information (ESI) available: High resolution ESI/MS spectra for **16**, **16a** and **16b**; HPLC traces and EPR spectra for compounds **5**, **6**, **8** - **11**; ^{1}H and ^{13}C NMR spectra for compounds **5a**, **6a**, **8a** - **11a**; HPLC traces and ^{1}H and ^{13}C NMR spectra for compounds **13**, **14** and **16.** For ESI see DOI: 10.1039/x0xx00000x

Organic & Biomolecular Chemistry Accepted Manuscript

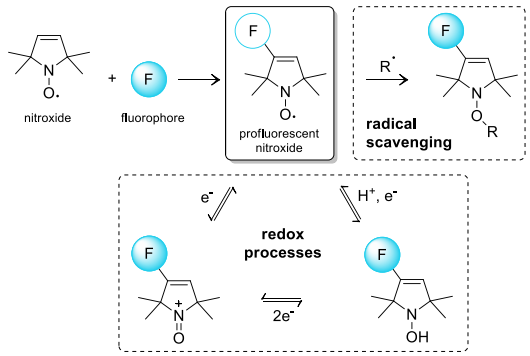

Fig. 1 A profluorescent nitroxide is typically synthesized from a nitroxide and a fluorophore. Fluorescence is restored via radical scavenging to the alkoxyamine or redox processes to the hydroxylamine or oxoammonium cation.

To elucidate the function of NO and the role of oxidative stress in biofilm formation and dispersal, it is prudent to develop methods to detect and visualize NO and the formation of free radicals associated with conditions of oxidative stress. Among the different techniques for monitoring free radicals, fluorescence techniques offer distinct advantages including high sensitivity, convenience and high spatiotemporal resolution when combined with laser-scanning confocal microscopy.[8] Most commercially available and bacteria-compatible viability imaging fluorescent probes fluoresce at long wavelengths which correspond to the red and green regions of the emission spectrum.[9] Such live/dead systems are well documented in biofilm microscopy and are often used qualitatively, for example to show cell death during the evacuation and lyse of a subpopulation of cells within microcolonies;[10] or to quantity cell viability in response to an introduced agent.[11] Furthermore, many free radical and NO probes in the literature emit in the green region of the spectrum making these probes incompatible with standard viability dyes systems.[12] In order to visualize oxidative stress and NO production simultaneously with live and dead cells and to minimize spectral overlap in a multi-dye system, fluorophores that emit at shorter wavelengths (440-490 nm), in the blue region of the spectrum, are desirable. Herein we report our work into the synthesis and visualization of two blue 'turn-on' fluorescent probes; i) a profluorescent nitroxide probe to detect free radical and redox processes associated with the generation of oxidative stress, and ii) a metal-based probe based on a coumarin scaffold to detect NO specifically.

Results and discussion

Free radical probe design and synthesis

Tethered nitroxide-fluorophore molecules (profluorescent nitroxides) are effective probes of free radical generation, reaction and associated changes in redox status that may occur during instances of oxidative stress within a biofilm.[13] Attachment of a nitroxide to a fluorophore leads to fluorescence quenching, which upon free radical scavenging,

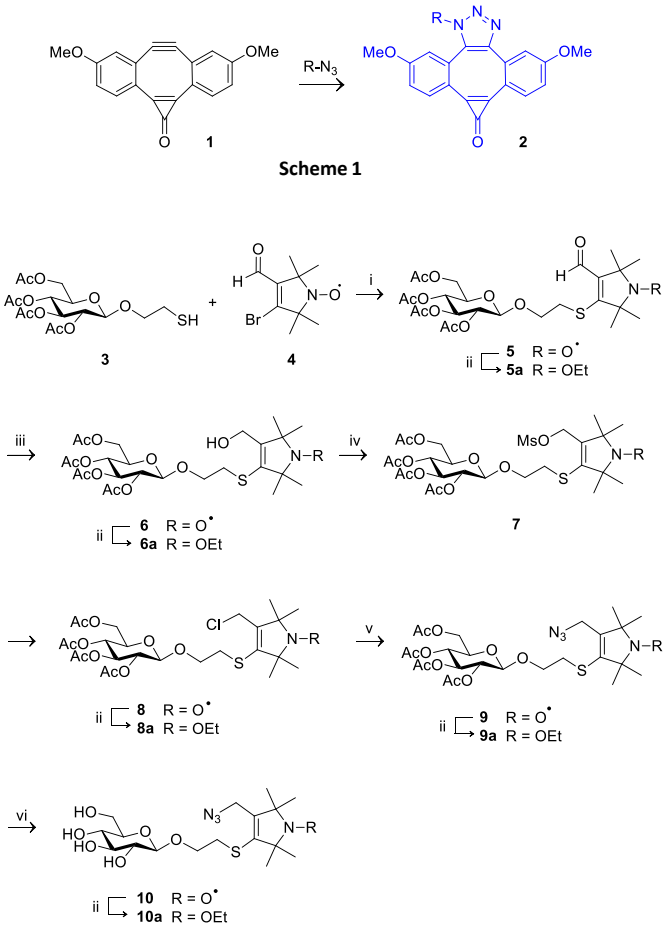

Scheme 2

Reagents and conditions: i) DBU, CH_3CN, 0°C to RT, 1 hr, 73%; ii) Et_3B, O_2, THF, 15 min, (**7a**,71%; **6a**, 82%; **8a**, 18%; **9a**, 67%; **10a**, 92%); iii) $NaBH_4$, EtOH, 0°C, 2 hr, 51%; iv) MsCl, Et_3N, CH_2Cl_2, 0 °C to RT, 1 hr, 94%; v) NaN_3, DMF, 100°C, 2 hr, 67%; vi) Na, CH_3OH, 0°C, 15 min, 94%.

metabolism or redox processes, returns the molecule to its native fluorescent state (Fig. 1).[14]

Blue fluorescent molecules currently on the market include but are not limited to, Cascade Blue, Lysosensor Blue, Marina Blue, Pacific Blue, 4',6-diamidino-2-phenylindole (DAPI) and Alexa Fluor 350 derivatives. However it was the dibenzocyclopropacyclooctynone **1** that drew our interest. Developed by Bertozzi and co-workers[15] and modified by Friscout, Fahrni and Boons,[16] the bridging triple bond of the modified dibenzocyclooctyne was found to undergo rapid, catalyst-free strain-promoted cycloaddition with azides to give triazole products that were in excess of 1300 times brighter fluorescence compared to the parent cyclooctyne (Scheme 1). We envisaged utilizing this moiety for the synthesis of a profluorescent nitroxide probe. Not only is the resultant triazole product **2** fluorescent in the desired blue spectral region, but installation of the nitroxide 'switch' through a triazole linkage is not only synthetically convenient but biologically stable in contrast to other commonly used linkage methods.[13]

Organic & Biomolecular Chemistry Accepted Manuscript

This journal is © The Royal Society of Chemistry 2015

With the **1**/**2** fluorescence system in mind, we began with the design of an azide that would undergo rapid, catalyst-free strain-promoted cycloaddition with dibenzocyclopropacyclooctynone **1** to give our final profluorescent nitroxide probe. In addition to the incorporation of the important redox-sensing nitroxide moiety into the azide partner, we were also interested in improving the water solubility and cell permeability of the highly organic alkyne **1** through the use of a hydrophilic carbohydrate substituent. The preparation of the azide partner **10** commenced by coupling thiol **3** and nitroxide **4** using 1,8-diazabicyclo-[5.4.0]undec-7-ene (DBU) as a non-nucleophilic base to give aldehyde **5** in 75% yield (Scheme 2). Aldehyde **5** was reduced carefully with sodium borohydride in anhydrous ethanol to give alcohol **6** in 51% yield. Reaction of alcohol **6** with methanesulfonyl chloride in the presence of triethylamine gave a mixture of mesylate **7** and chloride **8**. Increasing the number of equivalents of methanesulfonyl chloride resulted in the exclusive formation of **8** which was isolated in a near quantitative yield. Chloride **8** was then reacted with sodium azide in anhydrous *N,N*-dimethylformamide (DMF) to furnish the protected azide **9**. Deprotection with sodium methoxide gave the deprotected azide **10** as a yellow syrup. Due to the paramagnetic properties of nitroxides, NMR analysis of this class of compound typically results in peak broadening which limits the elucidation of detailed structural information. Glucosylnitroxides **5**, **6**, **8**, **9** and **10** were therefore characterized as their ethoxylamine derivatives (**5a**, **6a**, **8a**, **9a** and **10a**) using triethyl borane in the presence of oxygen.[17]

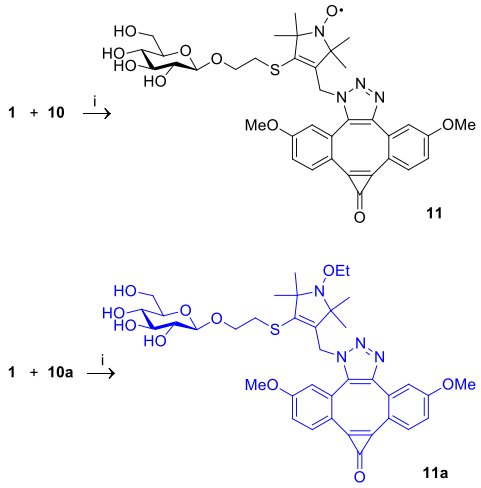

Scheme 3

Reagents and conditions: i) CH_2Cl_2/CH_3OH (4:1), RT, 32 hr, (**11**, 91%; **11a**, 81%).

Following the preparation of dibenzocyclooctyne **1**, which was synthesized by known procedures,[16] and with tri-functionalized azide **10** in hand, our attention turned to the final synthetic step towards the formation of our profluorescent nitroxide probe. Reaction of dibenzocyclooctyne **1** to its corresponding triazole product with azide **10** in 4:1 dichloromethane/methanol for 32 hours gave the novel profluorescent nitroxide probe **11** in 91% yield (Scheme 3). To measure the fluorometric properties of **11**, the ethoxylamine derivative **11a** was also synthesized.[18] Excitation of triazole **11a** at 360 nm produced a strong emission band centred at 484 nm. In contrast, excitation of the triazole **11** at 360 nm produced only a weak emission band indicating that the nitroxide moiety is an efficient quencher of fluorescence (Fig. 2).

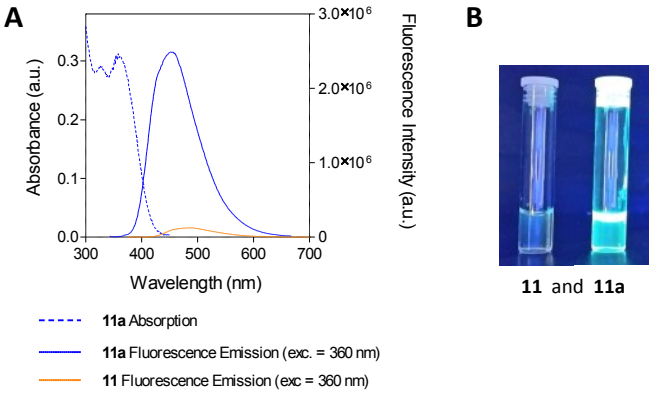

Fig. 2 A) Absorption (dashed blue trace) and emission (solid blue trace, λ_{ex} = 360 nm) spectra of triazole **11a**; and emission spectrum of triazole **11** (solid orange trace, λ_{ex} = 360 nm); all spectra recorded in CH_3OH at 10 μM; **B**) Image comparing the visible fluorescence emission of probe **11** (left vial, 10 μM in CH_3OH) and ethoxyamine **11a** (right vial, 10 μM in CH_3OH) under ultra violet (UV) excitation (365 nm).

NO probe design and synthesis

With the successful synthesis of a probe for the detection of free radical and redox processes, our attention turned to the synthesis of a blue NO-specific 'turn-on' probe. Metal-based fluorescent probes including those based on Co(II), Fe(II), Ru(II), Cu(II), or Rh(II)[9a, 19] are powerful probes to detect NO directly and specifically. In this strategy the close proximity of a transition metal can either quench the fluorescence of a pendant fluorophore until it reacts with NO or facilitate the reaction of NO with a dye component thereby restoring or 'switching-on' fluorescence.[20] Inspired by Lippard *et al.*,[9a] we envisaged coupling a coumarin-based scaffold to 2-methyl-8-aminoquinoline **15** in order to create, i) a metal-binding site for Cu(II) and fluorescence quenching, and ii) an active site for subsequent Cu(II) displacement by NO and the return of fluorescence.[21]

Organic & Biomolecular Chemistry Accepted Manuscript

Synthesis of the metal-complexed, coumarin-based probe began with the literature preparation of chlorobenzaldehyde **12**.[22] Subsequent reaction of chloride **12** with dimethyl malonate in the presence of pyridine and trace amount of acetic acid resulted in formation of coumarin **13** which was then formylated using a Duff reaction to give **14** in excellent yield (96%) (Scheme 4).[23] Aldehyde **14** was treated with quinoline **15**[24] in dichloromethane at room temperature to give an intermediate Schiff-base which was immediately reduced with sodium acetoxyborohyride to afford the final

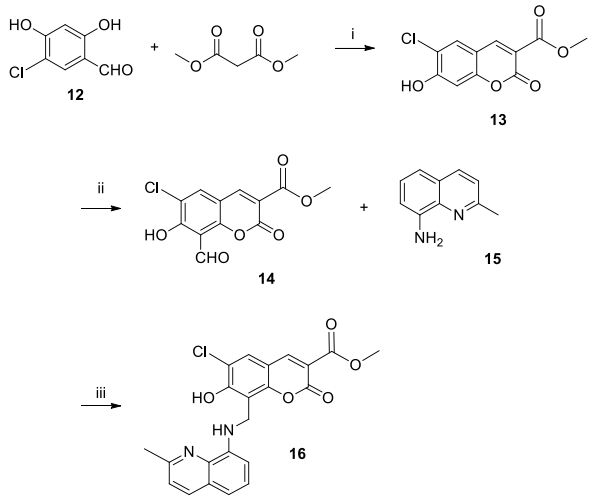

Scheme 4

Reagents and conditions: i) Piperidine, AcOH, EtOH, 60˚C, 6 hr, 50%; ii) Hexamine, TFA, reflux, 20 hr, 96%; iii) CH_3OH, CH_2Cl_2, 4Å molecular sieves, RT, 8 hr, then $Na(OAc)_3BH$, 24 hr, RT, 70%.

coumarin-based compound **16** in 70% yield over two steps.[25]

Fig. 3A shows the absorption and emission spectra of coumarin **16**. Excitation of **16** at 405 nm produced a strong emission band centered at 445 nm. Electrospray ionization mass spectrometry (ESI/MS) was used to monitor the treatment of **16** with a stoichiometrically equivalent amount of $CuCl_2$ which resulted in the formation of the Cu(II)-complexed coumarin **16a** (Scheme 5) (See ESI Fig. S1).† Excitation of **16a** at 405 nm (Fig. 3B) produced a weak emission band compared with that coumarin **16** suggesting that while the attachment of the paramagnetic Cu(II) ion does not result in compete fluorescence quenching, it is able to reduce the fluorescence of **16**. Subsequent reaction of **16a** with excess NO-donor, methylamine hexamethylene methylamine (MAHMA) NONOate, resulted in the displacement of Cu(II) by NO, forming the highly fluorescent **16b**, as confirmed by ESI/MS (see ESI Fig. S1).† The quantum yield calculations of **16a** and **16b** based on Coumarin 519/343 as a reference revealed that the probe is approximately 5 times more emissive in the presence of NO. To confirm the importance of the Cu(II)-complexed coumarin **16a** as an essential intermediate, **16** was reacted with excess MAHMA NONOate but no **16b** was observed by ESI/MS. Treatment of **16** with $NOBF_4$ (a source of NO^+) however, resulted in the successful formation of **16b** and

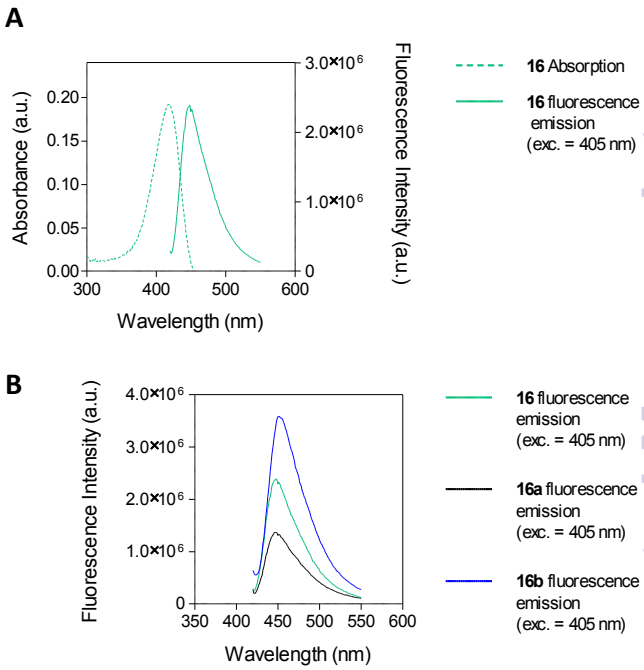

Fig. 3 A) Absorption (dashed green trace) and emission (solid green trace, λ_{ex} 405 nm) spectrum of coumarin **16**; **B**) Emission spectrum of **16** (solid green trace, λ_{ex} = 405 nm), **16a** (solid black trace, λ_{ex} = 405 nm), and **16b** (solid blue trace, λ_{ex} = 405 nm); all spectra recorded in TBS buffer (pH=7.6) and trace amount of DMSO at 25 µM.

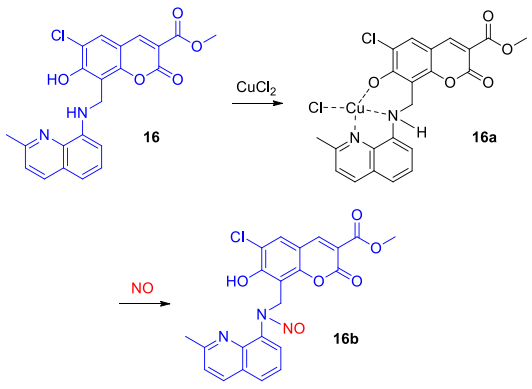

Scheme 5

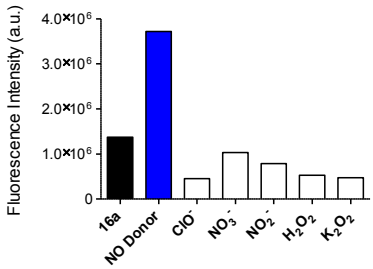

Fig. 4 Selectivity of **16a** fluorescence response for NO over other reactive nitrogen species.

Organic & Biomolecular Chemistry Accepted Manuscript

This journal is © The Royal Society of Chemistry 2015

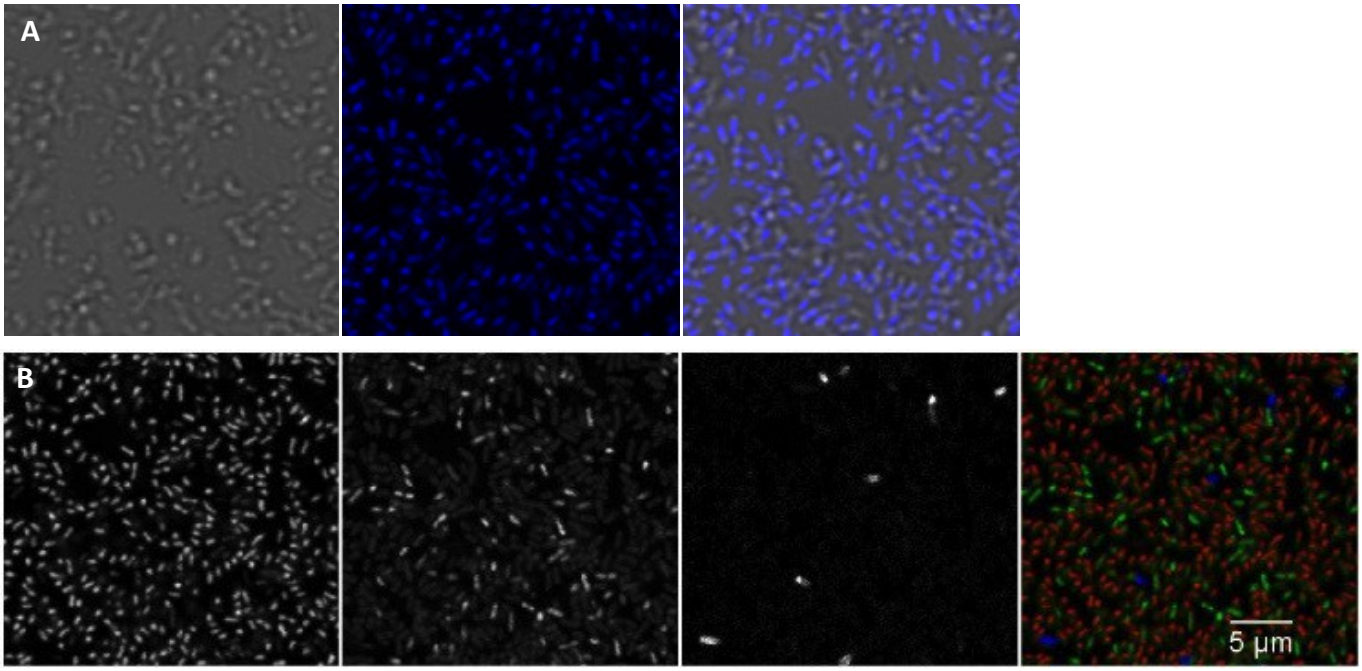

Fig. 5A Compound **11a** is cell permeable. Confocal photomicrographs of *P. aeruginosa* biofilms stained with **11a**. From left to right: light-field image; blue channel showing **11a** fluorescence; composite image. **B** Free radicals are generated predominately in live *P. aeruginosa* cells. Confocal photomicrographs separated into individual grey-scale channels. From left to right: red channel - propidium iodide (PI) stains dead cells; green channel - SYTO 9 stains live cells; blue channel – **11** detects free radical generation and reactions; colour composite image.

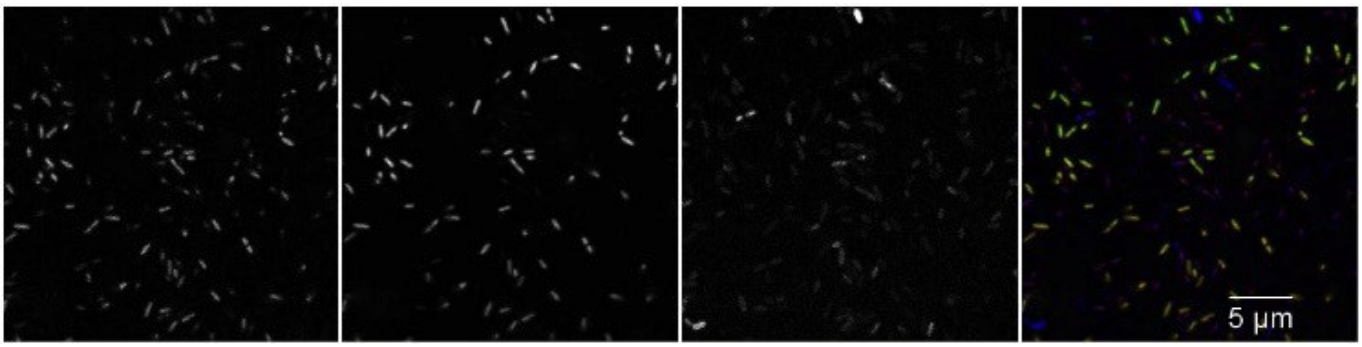

Fig. 6 NO is produced predominately in live *P. aeruginosa* cells. Confocal photomicrograph separated into individual grey-scale channels. From left to right: red channel - HCS NuclearMask™ Deep Red stain (HCS), stains DNA in both live cells and dead cells; green channel - PI, stains dead cells; blue channel – **16a** detects NO**;** colour composite image.

suggests that the electron accepting properties of Cu(II) are essential for NO-binding to the active site of **16**.

Next, the selectivity of the designed probe **16a** to NO was explored by investigating the fluorescence emission of **16a** in response to a selection of ROS and RNS. Fig. 4 reveals that the emission intensity of **16a** is unaffected by the reactive oxygen and nitrogen species tested (NO_2^-, NO_3^-, ClO^-, H_2O_2, and K_2O_2). These results suggest that **16a** is able to effectively and selectively bind NO.

Evaluation of blue probes 11 and 16a *in vivo* using confocal microscopy

Organic & Biomolecular Chemistry Accepted Manuscript

Following *in vitro* experiments, *in vivo* fluorescence imaging studies were carried out to investigate the ability of **11** and **16a** to detect free radical and redox processes and NO in bacterial cells. Twenty-four hour old biofilms of *P. aeruginosa* were stained with fluorescent reporter dyes and examined using confocal laser-scanning microscopy. As shown in the positive control experiments (Fig. 5A), the 'switched-on' ethoxylamine **11a** is highly cell-permeable with blue fluorescence co-localizing extensively with *P. aeruginosa* cells. When biofilms are stained with **11** (Fig. 5B), we observe blue fluorescence in a small percentage of cells, indicative of free radicals and redox processes occurring during biofilm growth. Likewise, **16b** fluorescence is observed in Fig. 6 indicating the presence of NO within cells. Co-localization calculations were performed by comparing the fluorescence intensity of the blue fluorophores in areas co-localized with live cells, dead cells and the EPM. The results shown in Fig. 7 indicate that in *P. aeruginosa* biofilms free radical generation and reaction occurs predominantly in live cells and in the EPM (Fig. 7A), and that NO is generated in live cells (Fig. 7B).

To the best of our knowledge, the results discussed above describe the first published example of the visualization and quantification of free radical generation and reaction in bacterial cells using a profluorescence nitroxide. Furthermore, as far as we are aware, it is also the first time NO has been successfully visualized in a bacterial cell using an NO-specific fluorescent probe.

Conclusions

Two novel fluorescent probes, which fluoresce in the blue spectral region (440-490 nm) and are compatible in multi-dye systems, were successfully synthesized. The first probe, a profluorescent nitroxide **11**, detects free radical and redox processes associated with oxidative stress during *P. aeruginosa* biofilm growth. The second, a Cu(II)-complexed coumarin-based NO probe **16a**, exhibits excellent selectivity and sensitivity for NO over other ROS and RNS and allows the visualization of NO within a biofilm. Co-localization studies

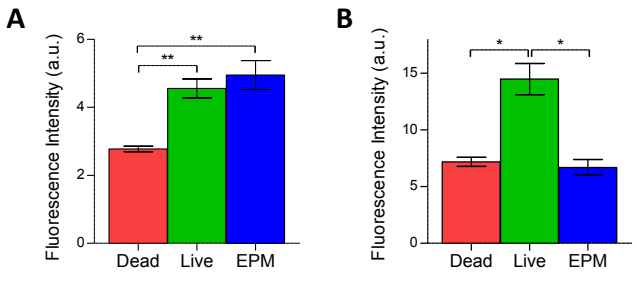

Fig. 7 Localization of free radical generation and reaction (**A**) and NO (**B**) in *P. aeruginosa* biofilms.

using digital image analysis revealed that conditions of oxidative stress and NO generation occur predominantly in live cells during normal biofilm growth as indicated by **11** and **16b** fluorescence respectively. Additional conditions of oxidative stress were also detected in the EPM using **11**.

The development of cell-permeable and bacteria-compatible probes **11** and **16a** has introduced two new microscopy tools for biofilm researchers. Their future use in experiments may provide further insight into the mechanistic detail of biofilm formation and dispersal, in particular the precise functions of ROS/RNS and NO during these biofilm events.

Experimental

3-[2-(2,3,4,6-Tetra-*O*-acetyl-β-D-glucopyranosyl)ethanethiyl]-4-formyl-2,2,5,5-tetramethyl-1-pyrrolinoxyl (5)

To a cooled (0°C) mixture of 3-bromo-4-formyl-2,2,5,5-tetramethyl-1-pyrrolinoxyl (**4**) (0.44 mmol, 107 mg) and 2,3,4,6-tetra-*O*-acetyl-1-(2-ethanethiol)-β-D-glucopyranoside (**3**) (0.44 mmol, 178 mg) in anhydrous CH_3CN (1.5 ml) was added DBU (0.48 mmol, 72 µl) drop-wise. After stirring at room temperature for 1 hour, the CH_3CN was removed *in vacuo* and the resulting residue was dissolved in EtOAc (10 ml) and washed with H_2O (2 x 5 ml). The organic phase was separated, dried ($MgSO_4$) and concentrated. Purification by flash column chromatography (hexane/EtOAc, 3:2) afforded the title compound **5** as a yellow solid (183 mg, 73%). R_f 0.23 (hexane/EtOAc, 3:2); MP 92-94°C; MS (ESI^+) *m/z* 597 $[M + Na]^+$; IR (neat): ν_{max} 2977, 1745, 1669, 1367, 1213, 1034, 907 cm^{-1}; $[\alpha]^{26}_{589}$ -3.7 (*c.* 0.8, $CHCl_3$); EPR (CH_2Cl_2): triplet, g = 2.0063, a_N = 14.74 G; HRMS (ESI^+) calc. For $C_{25}H_{36}NO_{12}SNa$ $[M + Na]^+$ 597.18504, found 597.19531; HPLC purity analysis: 98% pure, retention time: 16.6 min.

3-[2-(2,3,4,6-Tetra-*O*-acetyl-β-D-glucopyranosyl)ethanethiyl]-4-(hydroxymethyl)-2,2,5,5-tetramethyl-1-pyrrolinoxyl (6)

To a cooled (0°C) solution of **5** (3.86 mmol, 2.22 g) in anhydrous EtOH (250 ml) was added $NaBH_4$ (0.95 mmol, 36 mg) portion-wise. After stirring at 0°C for 1 hour, the solvent was removed *in vacuo* and the residue extracted into EtOAc (3 x 100 ml) and washed with H_2O (2 x 100 ml). The organic phase was dried ($MgSO_4$) and concentrated *in vacuo*. The residue was purified by flash column chromatography (EtOAc/hexane, 2:1) to give the title compound **6** as a yellow syrup (1.14 g, 51%). R_f 0.57 (EtOAc/hexane 2:1); MS (ESI^+) *m/z* 577 $[M + H]^+$; IR (neat): ν_{max} 3457, 2971, 1741, 1435, 1366, 1217, 1035, 906 cm^{-1}; $[\alpha]^{26}_{589}$ -14.4 (*c.* 0.8, $CHCl_3$); EPR (CH_2Cl_2): triplet, g = 2.0063, a_N = 14.06 G; HRMS (ESI^+) calc. for $C_{25}H_{39}NO_{12}S$ $[M + H]^+$ 577.21415, found 577.21448; HPLC purity analysis: 99 % pure, retention time: 20.2 min.

3-[2-(2,3,4,6-Tetra-*O*-acetyl-β-D-glucopyranosyl)ethanethiyl]-4-(chloromethyl)-2,2,5,5-tetramethyl-1-pyrrolinoxyl (8)

To a cooled (-10°C) solution of **6** (2.39 mmol, 1.38 g) and triethylamine (12.2 mmol, 1.7 ml) in CH_2Cl_2 (125 ml) was added methanesulfonyl chloride (5.49 mmol, 0.93 ml) drop-wise. The reaction was stirred at room temperature for 3 hours, washed

Organic & Biomolecular Chemistry Accepted Manuscript

This journal is © The Royal Society of Chemistry 2015

with H_2O (50 ml) and 5% aq. $NaHCO_3$ (50 ml). The organic phase was dried ($MgSO_4$), concentrated *in vacuo* and purified via flash chromatography (EtOAc/hexane gradient, 1:2, 1:1, 2:1) to afford the title compound **8** as a yellow syrup (1.35 g, 94%). R_f 0.56 (EtOAc/hexane, 2:1); MS (ESI^+) *m/z* 595 $[M + H]^+$; IR (neat): ν_{max} 2976, 1751, 1367, 1217, 1037, 907 cm^{-1}; $[\alpha]^{26}_{589}$ -4.2 (*c.* 0.9, $CHCl_3$); EPR (CH_2Cl_2): triplet, g = 2.0061, a_N = 14.35 G; HRMS (ESI^+) calc. for $C_{25}H_{39}ClNO_{11}S$ $[MH + H]^+$ 596.19269, found 596.19288; HPLC purity analysis: 98 % pure, retention time: 20.2 min.

3-[2-(2,3,4,6-Tetra-*O*-acetyl-β-D-glucopyranosyl)ethanethiyl]-4-(azidomethyl)-2,2,5,5-tetramethyl-1-pyrrolinoxyl (9)

Sodium azide (0.72 mmol, 47 mg) and **8** (0.60 mmol, 360 mg) were stirred in DMF (6 ml) for 2 hours at 100°C. The reaction mixture was diluted with Et_2O, washed with H_2O (3 x 3 ml) and the organic phase was dried ($MgSO_4$) and concentrated *in vacuo*. Purification via flash column chromatography (EtOAc/hexane gradient, 1:2, 1:1, 2:1) gave the title compound **9** as a yellow syrup (242 mg, 67%). R_f 0.59 (EtOAc/hexane, 2:1); MS (ESI^+) *m/z* 602 $[M + H]^+$; IR (neat): ν_{max} 2977, 2099, 1746, 1367, 1212, 1034, 906 cm^{-1}; $[\alpha]^{26}_{589}$ -7.8 (*c.* 0.8, $CHCl_3$); EPR (CH_2Cl_2): triplet, g = 2.0063, a_N = 14.36 G; HRMS (ESI^+) calc. for $C_{25}H_{37}N_4O_{11}SNa$ $[M + Na]^+$ 624.20717, found 624.20710; HPLC purity analysis: 97 % pure, retention time: 26.4 min.

4-(Azidomethyl)-3-(1-ethanethiyl-β-D-glucopyranosyl)-2,2,5,5-tetramethyl-1-pyrrolinoxyl (10)

To a cooled (0°C) solution of **9** (1.26 mmol, 759 mg) in anhydrous CH_3OH (20 ml) was added sodium metal (5.27 mmol, 122 mg) portion-wise. The solution was then stirred at room temperature for 15 minutes and quenched with Amberlite resin (H^+ form) until the solution was acidic (pH 1). The reaction mixture was filtered through celite, evaporated *in vacuo* and purified by flash column chromatography ($EtOAc/CH_3OH/H_2O$, 18:1:1) to afford the desired deprotected glycoside **10** as a yellow syrup (493 mg, 94%). R_f 0.29 ($EtOAc/CH_3OH/H_2O$, 18:1:1); MS (ESI^+) *m/z* 434 $[M + H]^+$; IR (neat): ν_{max} 3367, 2931, 2098, 1072, 1016 cm^{-1}; $[\alpha]^{27}_{589}$ -14.0 (*c.* 0.7, CH_3OH); EPR (CH_2Cl_2): triplet, g = 2.0063, a_N = 14.16 G; HRMS (ESI^+) calc. for $C_{17}H_{29}N_4O_7SNa$ $[M + Na]^+$ 456.16492, found 456.16492; HPLC purity analysis: >99% pure, retention time: 12.4 min.

3-[2-(2,3,4,6-Tetra-*O*-acetyl-β-D-glucopyranosyl)ethanethiyl]-1-ethoxy-4-formyl-2,2,5,5-tetramethylpyrroline (5a)

To a solution of nitroxide **5** (38.3 µmol, 22 mg) in anhydrous THF (0.5 ml) was added triethylborane (1.0 M in THF, 46 µl). The solution was allowed to stir under a saturated oxygen atmosphere for 15 minutes. The reaction mixture was concentrated *in vacuo*, and purified by flash column chromatography (EtOAc/hexane gradient, 1:2, 1:1, 2:1) to afford the title compound **5a** as a colourless syrup (16.5 mg, 71%). R_f 0.70 (EtOAc/hexane 2:1); MS (ESI^+) *m/z* 604 $[M + H]^+$; IR (neat): ν_{max} 2917, 2849, 1741, 1467, 1366, 1229, 1217, 1043, 718 cm^{-1}; ^1H NMR ($CDCl_3$, 500 MHz): δ_H 10.03 (1H, s), 5.20 (1H, t, *J* = 9.5 Hz), 5.08 (1H, t, *J* = 9.7 Hz), 4.99 (1H, dd, *J* = 8.0, 9.7 Hz), 4.52 (1H, d, *J* = 8.0 Hz), 4.24 (1H, dd, *J* = 4.7, 12.4 Hz), 4.14 (1H, dd, *J* = 2.4, 12.3 Hz), 4.00 (1H, dt, *J* = 5.2, 10.4 Hz), 3.86 (2H, q, *J* = 7.1, 14.2 Hz), 3.71-3.65 (2H, m), 3.11-3.02 (2H, m), 2.09, 2.06, 2.02, 2.00 (12H, 4s), 1.35 (12H, br s), 1.19 (3H, t, *J* = 7.1 Hz); ^{13}C NMR ($CDCl_3$, 125 MHz): δ_C 188.7, 170.8, 170.4, 169.5, 169.4, 158.9, 145.2, 100.8, 73.0, 72.83, 72.77, 72.1, 71.2, 68.9, 68.4, 68.2, 62.0, 36.1, 20.9, 20.84, 20.75, 20.7, 14.5; HRMS (ESI^+) calc. for $C_{27}H_{42}NO_{12}S$ $[M + H]^+$ 604.24222, found 604.24223.

3-[2-(2,3,4,6-Tetra-*O*-acetyl-β-D-glucopyranosyl)ethanethiyl]-4-(hydroxymethyl)-1-ethoxy-2,2,5,5-tetramethylpyrroline (6a)

Compound **6a** was prepared by using the procedure described for **5a** above. Nitroxide **6** (20.1 µmol, 12 mg) and triethylborane (1.0 M in THF, 60 µl) in THF (1 ml) followed by flash column chromatography (EtOAc/hexane gradient, 1:2, 1:1, 2:1) afforded the title compound **6a** as a colourless syrup (10 mg, 82%). R_f 0.66 (EtOAc/hexane 2:1); MS (ESI^+) *m/z* 606 $[M + H]^+$; IR (neat): ν_{max} 3500, 2975, 1749, 1368, 1215, 1037, 907 cm^{-1}; ^1H NMR ($CDCl_3$, 400 MHz): δ_H 5.21 (1H, t, *J* = 9.5 Hz), 5.08 (1H, t, *J* = 9.4 Hz), 5.00 (1H, t, *J* = 8.8 Hz), 4.56 (1H, d, *J* = 8.0 Hz), 4.32 (2H, br s), 4.24 (1H, dd, *J* = 4.6, 12.4 Hz), 4.16-4.09 (1H, m), 3.97 (1H, dt, *J* = 5.7, 10.4 Hz), 3.85 (2H, q, *J* = 7.0, 14.1 Hz), 3.71-3.66 (2H, m), 2.92-2.81 (2H, m), 2.35 (1H, br s), 2.09, 2.07, 2.02, 2.01 (12H, 4s), 1.27, 1.25 (12H, 2s), 1.19 (3H, t, *J* = 7.1 Hz); ^{13}C NMR ($CDCl_3$, 100 MHz): δ_C 170.9, 170.4, 169.6, 169.5, 151.7, 134.1, 100.7, 72.9, 72.6, 72.1, 71.7, 71.3, 69.8, 68.5, 68.2, 62.0, 58.0, 35.1, 20.90, 20.89, 20.8, 20.7, 14.6; HRMS (ESI^+) calc. for $C_{27}H_{44}NO_{12}S$ $[M + H]^+$ 604.246.25787, found 606.25790.

3-[2-(2,3,4,6-Tetra-*O*-acetyl-β-D-glucopyranosyl)ethanethiyl]-4-(chloromethyl)-1-ethoxy-2,2,5,5-tetramethylpyrroline (8a)

Compound **8a** was prepared by using the procedure described for **5a** above. Nitroxide **8** (16.8 µmol, 10 mg) and triethylborane (1.0 M in THF, 50 µl) in THF (1 ml) followed by flash column chromatography (EtOAc/hexane gradient, 1:2, 1:1, 2:1) afforded the title compound **8a** as a colourless syrup (1.9 mg, 18%). R_f 0.69 (EtOAc/hexane 2:1); MS (ESI^+) *m/z* 624 $[M + H]^+$; ^1H NMR ($CDCl_3$, 500 MHz): δ_H 5.21 (1H, t, *J* = 9.5 Hz), 5.08 (1H, t, *J* = 9.7 Hz), 5.00 (1H, dd, *J* = 8.0, 9.6 Hz), 4.57 (1H, d, *J* = 8.0 Hz), 4.32 (2H, br s), 4.24 (1H, dd, *J* = 4.7, 12.4 Hz), 4.15 (1H, dd, *J* = 2.5, 12.3 Hz), 3.97 (1H, dt, *J* = 6.2, 10.5 Hz), 3.86 (2H, q, *J* = 7.1, 14.2 Hz), 3.72-3.67 (2H, m), 2.91-2.82 (2H, m), 2.09, 2.07, 2.02, 2.00 (12H, 4s), 1.28, 1.25 (12H, 2s), 1.19 (3H, t, *J* = 7.1 Hz); ^{13}C NMR ($CDCl_3$, 125 MHz): δ_C 170.8, 170.4, 169.6, 169.5, 151.7, 134.1, 100.7, 72.9, 72.6, 72.1, 71.7, 71.3, 69.8, 68.5, 68.2, 62.0, 58.0, 35.1, 20.92, 20.90, 20.77, 20.75, 14.6.

3-[2-(2,3,4,6-Tetra-*O*-acetyl-β-D-glucopyranosyl)ethanethiyl]-4-(azidomethyl)-1-ethoxy-2,2,5,5-tetramethylpyrroline (9a)

Organic & Biomolecular Chemistry Accepted Manuscript

Compound **9a** was prepared by using the procedure described for **5a** above. Nitroxide **9** (38.2 µmol, 23 mg) and triethylborane (1.0 M in THF, 115 µl) in THF (2 ml) followed by flash column chromatography (EtOAc/hexane gradient, 1:2, 1:1, 2:1) afforded the title compound **9a** as a colourless syrup (16.2 mg, 67%). R_f 0.89 (EtOAc/hexane 2:1); MS (ESI^+) *m/z* 631 $[M + H]^+$; IR (neat): ν_{max} 2972, 2099, 1749, 1366, 1213, 1034, 908 cm^{-1}; ^1H NMR ($CDCl_3$, 500 MHz): δ_H 5.20 (1H, t, *J* = 9.5 Hz), 5.08 (1H, t, *J* = 9.7 Hz), 4.99 (1H, dd, *J* = 8.0, 9.7 Hz), 4.53 (1H, d, *J* = 8.0 Hz), 4.25 (1H, dd, *J* = 7.1 Hz), 3.96 (2H, dt, *J* = 6.3, 10.4 Hz), 3.85 (2H, q, *J* = 7.1, 14.2 Hz), 3.69 (1H, ddd, *J* = 2.4, 4.7, 10.0 Hz), 3.66 (1H, dt, *J* = 7.0, 10.4Hz), 2.90-2.79 (2H, m), 2.08, 2.06, 2.02, 2.00 (12H, 4s), 1.28, 1.27 (12H, 2s)m 1.19 (3H, t, *J* = 7.1 Hz); ^{13}C NMR ($CDCl_3$, 125 MHz): δ_C 170.8, 170.4, 169.51, 169.47, 146.0, 139.3, 100.8, 72.9, 72.7, 72.1, 71.9, 71.2, 69.3, 68.6, 68.5, 62.0, 46.3, 35.2, 20.88, 20.85, 20.8, 20.7, 14.6; HRMS (ESI^+) calc. for $C_{27}H_{43}N_4O_{11}S$ $[M + H]^+$ 631.26436, found 631.26520.

4-(Azidomethyl)-3-(1-ethanethiyl-β-D-glucopyranosyl)-1-ethoxy-2,2,5,5-tetramethylpyrroline (10a)

Compound **10a** was prepared by using the procedure described for **5a** above. Nitroxide **10** (42.0 µmol, 18 mg) and triethylborane (1.0 M in THF, 126 µl) in THF (2 ml) followed by flash column chromatography (EtOAc/CH_3OH/H_2O, 18:1:1) afforded the title compound **10a** as a colourless syrup (17.9 mg, 92%). R_f 0.30 (EtOAc/CH_3OH/H_2O, 18:1:1); MS (ESI^+) *m/z* 463 $[M + H]^+$; IR (neat): ν_{max} 3368, 2971, 2096, 1021 cm^{-1}; ^1H NMR (CD_3OD, 500 MHz): δ_H 4.28 (1H, d, *J* = 3.9 Hz), 4.12 (2H, br s), 3.97 (1H, dt, *J* = 6.9, 10.4 Hz), 3.88 (2H, q, *J* = 7.1, 14.3 Hz), 3.85 (1H, d, *J* = 2.0 Hz), 3.72 (1H, dt, *J* = 6.8, 10.4 Hz), 3.67 (1H, dd, *J* = 5.3, 11.8 Hz), 3.35 (1H, t, *J* = 8.8 Hz), 3.29-3.24 (2H, m), 3.19 (1H, dd, *J* = 7.9, 9.0 Hz), 2.93 (2H, td, *J* = 1.0, 6.8 Hz), 1.31, 1.29 (12H, 2s), 1.19 (3H, t, *J* = 7.1 Hz), ^{13}C NMR (CD_3OD, 125 MHz): δ_C 147.2, 140.6, 104.4, 78.03, 77.96, 75.0, 73.5, 73.0, 71.6, 70.5, 69.4, 62.7, 47.1, 36.0, 29.1 (br), 23.1 (br), 14.7; HRMS (ESI^+) calc. for $C_{19}H_{35}N_4O_7S$ $[M + H]^+$ 463.22210, found 463.22211.

4-(5,11-Dimethoxy-8-oxodibenzo[3,4:7,8]cyclopropa[5,6]cycloocta[1,2-*d*][1,2,3]triazol-1(8*H*)-yl)methyl-3-(1-ethanethiyl-β-D-glucopyranosyl)-2,2,5,5-tetramethyl-1-pyrrolinoxyl (11)

A solution of 4,9-dimethoxy-6,7-didehydro-1*H*-dibenzo[*a,e*]cyclopropa[*c*]cycloocten-1-one (**1**) (0.29 mmol, 84 mg) and 4-azidomethyl-3-(1-ethanethiyl-β-D-glucopyranosyl)-2,2,5,5-tetramethyl-1-pyrrolinoxyl (**10**) (0.58 mmol, 253 mg) in a mixture of CH_2Cl_2 and CH_3OH (4:1, 25 ml) was stirred at room temperature for 32 hours. The solvent was then removed *in vacuo* and purified by preparatory TLC (EtOAc/CH_3OH/H_2O, 18:1:1) to furnish the compound **11** as a yellow powder (191 mg, 91%). R_f 0.29 (EtOAc/CH_3OH/H_2O, 18:1:1); MP 154-156°C; MS (ESI^+) *m/z* 722 $[M + H]^+$; IR ν_{max} 3355, 2924, 1854, 1600, 1227, 1022 cm^{-1}; $[\alpha]^{24}_{589}$ -8.6 (*c.* 1.3, CH_3OH); EPR (CH_2Cl_2): triplet, g = 2.0061, a_N = 15.92 G; HRMS (ESI^+) calc. for $C_{36}H_{42}N_4O_{10}S$ 722.26162 $[M + H]^+$, found 722.26165; HPLC purity analysis: >99% pure, retention time: 15.9 min; UV-vis: λ_{max} (10 µM in CH_3OH) 360, 328 nm (ε. 3299, 3499 L mol^{-1} cm^{-1}); Fluorescence emission (λ_{ex} 360 nm): λ_{max} = 484 nm (10 µM in CH_3OH).

4-(5,11-Dimethoxy-8-oxodibenzo[3,4:7,8]cyclopropa[5,6]cycloocta[1,2-*d*][1,2,3]triazol-1(8*H*)-yl)methyl-3-(1-ethanethiyl-β-D-glucopyranosyl)-1-ethoxy-2,2,5,5-tetramethylpyrroline (11a)

Compound **11a** was prepared by using the procedure described for **11** above. 4,9-Dimethoxy-6,7-didehydro-1*H*-dibenzo[*a,e*]cyclopropa[*c*]cycloocten-1-one (**1**) (0.17 mmol, 47 mg) and 4-azidomethyl-3-(1-ethanethiyl-β-D-glucopyranosyl)-1-ethoxy-2,2,5,5-tetramethyl pyrroline (**10a**) (0.34 mmol, 156 mg) in CH_2Cl_2/CH_3OH (4:1, 25 ml) followed by preparatory TLC (EtOAc/CH_3OH/H_2O, 18:1:1) afforded compound **11a** as a yellow powder (200 mg, 81%). R_f 0.23 (EtOAc/CH_3OH/H_2O, 18:1:1); MP 228-230°C (dec.); MS (ESI^+) *m/z* 751 $[M + H]^+$; IR ν_{max} 3681, 3353, 2974, 2866, 2076, 1882, 1598, 1564, 1455, 1346, 1226, 1056, 1015, 1033, 821 cm^{-1}; $[\alpha]^{23}_{589}$ -5.7 (*c.* 1.1, CH_3OH); ^1H NMR ($CDCl_3$, 700 MHz): δ_H 7.60-7.52 (2H, m), 7.33 (1H, br s), 6.96-6.90 (3H, m), 5.34 (2H, dd, *J* = 14.7, 24.1 Hz), 4.97 (1H, s), 4.82 (1H, s), 4.51 (1H, s), 4.32 (1H, dd, *J* = 6.9, 15.7 Hz), 3.89 (3H, s), 3.86 (3H, s), 3.71 (2H, dd, *J* = 7.1, 13.8 Hz), 3.68-3.61 (3H, m), 3.30-3.37 (2H, m), 2.77 (2H, s), 1.13 (6H, s), 1.08 (3H, t *J* = 7.1 Hz), 0.96 (3H, s), 0.74 (3H, s); ^{13}C NMR ($CDCl_3$, 125 MHz): δ_C 163.3, 162.9, 152.7, 151.7, 149.8, 144.8, 143.3, 138.5, 137.9, 135.7, 133.7, 130.0, 119.6, 118.7, 117.6, 117.0, 115.2, 130.0, 102.8, 76.6, 76.5, 75.9, 73.7, 72.6, 72.0, 71.9, 69.8, 69.2, 62.7, 61.6, 56.1, 55.9, 35.2, 28.2 (br), 22.5 (br), 14.5; HRMS (ESI^+) calc. for $C_{38}H_{46}N_4O_{10}SNa$ 773.28269 $[M + Na]^+$, found 773.28268; HPLC purity analysis: 99% pure, retention time: 20.7 min; UV-vis: λ_{max} (10 µM in CH_3OH) 360, 328 nm (ε. 6481, 6017 L mol^{-1} cm^{-1}); Fluorescence emission (λ_{ex} 360 nm): λ_{max} = 484 nm (10 µM in CH_3OH).

Methyl-6-chloro-7-hydroxy-2-oxo-2*H*-chromene-3-carboxylate (13).

To 5-chloro-2,4-dihydroxybenzaldehyde (**12**) (3.13 g, 18 mmol) and dimethyl malonate (2.6 g, 19.3 mmol) in CH_3OH (42 ml) was added piperidine (0.2 ml, 1.8 mmol) and glacial acetic acid (0.1 ml). The reaction mixture was heated under reflux for 7 hours to afford the title coumarin **13** as a precipitate without further purification (2.3 g, 50%). R_f 0.27 (EtOAc/hexane, 70:30); MS (ESI^+) *m/z* 253.03 $[M + H]^+$; IR ν_{max} 3241, 1619, 1581, 1192, 719 cm^{-1}; ^{1}HNMR (dimethyl sulfoxide (DMSO)-d_6, 400 MHz): δ_H 8.66 (s, 1H), 7.99 (s, 1H), 6.87 (s, 1H), 3.78 (s, 3H); ^{13}C NMR (400 MHz, DMSO-d_6): δ_C 163.7, 159.5, 156.0, 155.8, 149.2, 131.3, 118.3, 113.2, 111.1, 103.3, 52.7. HRMS (ESI^+) calc. for $C_{11}H_7ClO_5Na$ 276.98742 $[M + Na]^+$, found 276.98699. HPLC purity analysis: 88% pure, retention time: 9.74 min.

Methyl-6-chloro-7-hydroxy-8-formyl-coumarin-3-carboxylate (14):

Organic & Biomolecular Chemistry Accepted Manuscript

This journal is © The Royal Society of Chemistry 2015

A solution of **13** (750 mg, 2.94 mmol) and hexamine (618 mg, 4.41 mmol) in trifluoroacetic acid (TFA) (6 ml) was heated under reflux for 20 hours. H_2O (60 ml) was added and the solution was stirred for a further 30 minutes at 60°C. After cooling, the precipitate was collected by filtration to give the title compound **14** as a yellow solid (0.8 g, 96%). R_f 0.20 (EtOAc/hexane, 70:30); MS (ESI^+) *m/z* 281.03 $[M + H]^+$; IR ν_{max} 2981, 1737, 1439, 1233, 791 cm^{-1}; ^{1}HNMR (DMSO-d_6, 400 MHz): δ_H 10.36 (s, 1H), 8.71 (s, 1H), 8.30 (s, 1H), 3.81 (s, 1H); ^{13}C NMR (400 MHz, DMSO-d_6): δ_C 190.4, 163.3, 157.9, 152.9, 148.5, 130.5, 127.0, 111.1, 110.4, 100.7, 52.8; HRMS (ESI^+) calc. for $C_{12}H_7ClO_6Na$ 304.98234 $[M + Na]^+$, found 304.98168. HPLC purity analysis: >99% pure, retention time: 10.98 min.

Methyl-6-Chloro-7-hydroxy-8-(2-methylquinaldine)-coumarin-3-carboxylate (16):

To a stirred solution of **14** (50 mg, 0.177 mmol) and 4Å molecular sieves in dry CH_2Cl_2 (15 ml) was added a solution of 8-aminoquinoline (**15**) (31 mg, 0.194 mmol) in dry CH_3OH (10 ml). The mixture was stirred at room temperature for 2 hours. The reaction mixture was then cooled to 0°C, sodium triacetoxyborohydride (75 mg, 0.354 mmol) was added portion-wise. After warming to room temperature and stirring overnight the crude material was purified by flash column chromatography (CH_3OH/CH_2Cl_2, 0:1 then 1:100) to afford the title compound **16** as a yellow solid (52 mg, 70%). R_f 0.5 (EtOAc/hexane, 3:2); MS (ESI^+) *m/z* 425.10 $[M + H]^+$; IR ν_{max} 3443, 2981, 1659, 1436, 1406, 1023 cm^{-1}; ^{1}H NMR (500 MHz, DMSO-d_6): δ_H 8.65 (1H, s), 8.05 (1H, d, *J* = 7Hz), 7.95 (1H, s), 7.3 3 (1H, d, *J* = 7Hz), 7.25 (1H, t, *J* = 7Hz), 7.02 (1H, d, *J* = 7Hz), 6.89 (1H, d, *J* = 10Hz), 4.63(2H, s), 3.78(3H, s), 2.58(s, 3H); ^{13}C NMR (500 MHz, DMSO-d_6): δ_C 163.6, 157.9, 157.2, 156.3, 156.2, 154.3, 154.1, 149.5, 149.4, 130.8, 127.1, 129.4, 125.8, 124.9, 123.0, 118.6, 114.0, 113.8, 112.0,111.7, 52.6, 35.5, 25.2; HPLC purity analysis: >99% pure, retention time: 12.16 min.

MS analysis of 16, 16a and 16b

*Preparation of **16, 16a** and **16b.*** **16** was prepared as a 1 mM stock solution in CH_3CN and diluted to a final concentration of 25 µM with tris buffered saline (TBS). **16a** was prepared from **16** (500 µl, 1 mM in CH_3CN) and $CuCl_2$ (500 µl, 1 mM in H_2O) and then diluted to a final concentration of 50 µM with TBS. MAHMA NONOate was prepared as a 25 mM stock with NaOH (1 mM in H_2O) and then diluted to a final concentration of 5 mM with TBS. **16b** was prepared by adding MAHMA NONOate (500 µl, 5 mM) to **16a** (500 µl, 50 µM). This solution was allowed to stand at room temperature for 30 minutes without stirring. **16b** was also prepared from **16** (500 µl, 1 mM in CH_3CN) and $NOBF_4$ (500 µl, 4 mM in CH_3CN), and stirred at room temperature for 15 minutes.

MS analysis. MS experiments on **16**, **16a** and **16b** were carried out using a Finnigan hybrid linear quadrupole transform ion-cyclotron resonance (LTQ FTICR) mass spectrometer. Solutions were drawn into a 500 µl gas tight borosilicate glass syringe with PTFE plunger tips and injected into the Finnigan ESI source at 5 µl.min^{-1}. ESI source conditions to yield a stable spray current of 0.5 µA were: needle potential (5.0 kV); nitrogen sheath gas pressure (8 arbitrary units). The ion transfer capillary temperature was set to 275°C. Voltages were: tube lens (30 V) and capillary voltage (100 V).

16: HRMS (ESI^+) calc. for $C_{22}H_{18}ClN_2O_5$ 425.08988 $[M + H]^+$, found 425.08908; **16a**: HRMS (ESI^+) calc. for $C_{22}H_{17}ClCuN_2O_5$ 487.01165 $[M - Cl + H]^+$, found 487.01154; **16b**: HRMS (ESI^+) calc. for $C_{22}H_{17}ClN_3O_6$ 454.080044 $[M + H]^+$, found 545.07992 (see ESI, Fig. S1).†

General procedure for confocal microscopy and co-localization calculations for probes 11 and 16a

Overnight cultures of *P. aeruginosa* were diluted 100-fold in M9 minimal media and inoculated (100 µl per well) in a µ-slide 8-well microscopy chamber (Ibidi). The chamber was incubated for 24 hours at ambient temperatures (19-22°C). After incubation, the resultant biofilms within the wells were treated with probes (**11 or 16a**) and live/dead cells stains. Images were collected with Leica LAS AF software and formatted with ImageJ. Volocity (PerkinElmer) was used to digitally analyse fluorescence images. Co-localization calculations were performed by classifying and counting fluorescence specific pixels in the blue channel (in which probes fluoresce) in areas co-localized with live cells, dead cells and the EPM. Pixels were classified and counted on the basis of their relative fluorescence density compared with the background via a threshold process. This analysis was performed on at least four images on each sample from different locations of the bacterial microcolonies comprising 2 independent experiments.

Confocal microscopy and co-localization calculations with profluorescent nitroxide probe 11

Profluorescent nitroxide probe **11** was prepared as a 2 mM stock in DMSO and diluted to 100 µM with TBS for cell staining. The LIVE/DEAD BacLight viability kit (Molecular Probes™) consisted of SYTO 9 and propidium iodide (PI). SYTO 9, available as a 5 mM stock in DMSO, was used at a final concentration of 5 µM in TBS; and PI, available as a 1.5 mM stock in distilled H_2O, was used at a final concentration of 30 µM in TBS. The resultant biofilms within the wells were treated with profluorescent nitroxide probe **11** (100 µM in TBS) for 1 hour in the dark, rinsed with TBS (2 x 100 µl) and stained with SYTO 9 and PI for 15 minutes in the dark. 'Switched on' **11**, live cells and dead cells were visualized with a Leica SP5 Inverted laser scanning microscope with a 405 laser (405 nm), an argon laser (488 nm) and a Helium-Neon (633 nm) and respectively. Representative images depicted in Fig. 5; ** denote statistically significant differences compared to **11** fluorescence within dead cells where $p<0.01$ (Mann-Whitney t-test: two-tailed, unpaired, equal variance, n = 4); error bars indicate standard deviation.

Organic & Biomolecular Chemistry Accepted Manuscript

Confocal microscopy and co-localization calculations with NO probe 16a

NO probe **16** was prepared as a 1 mM stock in DMSO and diluted to 10 μM with TBS for cell staining. The live/dead staining system used consisted of HCS NuclearMask^{TM} Deep Red stain (HCS) (Molecular Probes^{TM}) and PI. HCS, available as a 250x concentrate in DMSO was diluted 1/250 in TBS; and PI, available as a 750 μM stock in distilled H_2O and DMSO (1:1), was used at a final concentration of 4.5 μM in TBS. The resultant biofilms within the wells were first treated with KNO_3 for 3 hours at 37°C to induce NO production by *P. aeruginosa* cells. The cells, while protected from light, were then treated with a freshly prepared solution of **16a** (1:1 solution of $CuCl_2$ and **16**, 10 μM in TBS, 1 hour), rinsed with TBS (2 x 100 μl), stained with HCS (30 minutes) and then PI (15 minutes) in the dark. **16b**, PI and HCS were visualized with a Leica SP5 Inverted laser scanning microscope with a 405 laser (405 nm), Diode-Pumped Solid-State laser (561) and Helium-Neon laser (633 nm) respectively. Representative images depicted in Fig. 6; * denote statistically significant differences compared to **16b** fluorescence within dead cells where $p<0.05$ (Mann-Whitney t-test: two-tailed, unpaired, equal variance, n = 4); error bars indicate standard deviation.

Acknowledgements

We thank the Australian Research Council through the Centres of Excellence Scheme and the Albert Shimmins Memorial Fund for generous support.

References

1. (a) O. Ciferri, *Appl. Environ. Microbiol.*, 1999, **65**, 879; (b) M. Kostakioti, M. Hadjifrangiskou and S. J. Hultgren, *Cold Spring Harb. Perspect. Med.*, 2013, **3**, a010306.
2. J. W. Costerton, P. S. Stewart and E. P. Greenberg, *Science*, 1999, **284**, 1318.
3. D. McDougald, S. A. Rice, N. Barraud, P. D. Steinberg and S. Kjelleberg, *Nat. Rev. Micro.*, 2012, **10**, 39.
4. R. J. Worthington, J. J. Richards and C. Melander, *Org. Biomol. Chem.*, 2012, **10**, 7457.
5. (a) N. Barraud, D. J. Hassett, S.-H. Hwang, S. A. Rice, S. Kjelleberg and J. S. Webb, *J. Bacteriol.*, 2006, **188**, 7344; (b) N. Barraud, D. Schleheck, J. Klebensberger, J. S. Webb, D. J. Hassett, S. A. Rice and S. Kjelleberg, *J. Bacteriol.*, 2009, **191**, 7333; (c) N. Liu, Y. Xu, S. Hossain, N. Huang, D. Coursolle, J. A. Gralnick and E. M. Boon, *Biochemistry*, 2012, **51**, 2087.
6. N. R. Yepuri, N. Barraud, N. S. Mohammadi, B. G. Kardak, S. Kjelleberg, S. A. Rice and M. J. Kelso, *Chem. Commun.*, 2013, **49**, 4791.
7. (a) S.-A. Alexander, C. Kyi and C. H. Schiesser, *Org. Biomol. Chem.*, 2015, **13**, 4751; (b) S.-A. Alexander, E. M. Rouse, J. M. White, N. Tse, C. Kyi and C. H. Schiesser, *Chem. Commun.*, 2015, **51**, 3355.
8. M. Barzegar Amiri Olia, C. H. Schiesser and M. K. Taylor, *Org. Biomol. Chem.*, 2014, **12**, 6757.
9. (a) U.-P. Apfel, D. Buccella, J. J. Wilson and S. J. Lippard, *Inorg. Chem.*, 2013, **52**, 3285; (b) G. K. Vegesna, S. R. Sripathi, J. Zhang, S. Zhu, W. He, F.-T. Luo, W. J. Jahng, M. Frost and H. Liu, *ACS Appl. Mater. Inter.*, 2013, **5**, 4107; (c) T.-W. Shiue, Y.-H. Chen, C.-M. Wu, G. Singh, H.-Y. Chen, C.-H. Hung, W.-F. Liaw and Y.-M. Wang, *Inorg. Chem.*, 2012, **51**, 5400.
10. (a) K. Sauer, A. K. Camper, G. D. Ehrlich, J. W. Costerton and D. G. Davies, *J. Bacteriol.*, 2002, **184**, 1140; (b) S. M. Hunt, E. M. Werner, B. Huang, M. A. Hamilton and P. S. Stewart, *Appl. Environ. Microbiol.*, 2004, **70**, 7418; (c) B. Purevdorj-Gage, W. J. Costerton and P. Stoodley, *Microbiol.*, 2005, **151**, 1569; (d) J. S. Webb, L. S. Thompson, S. James, T. Charlton, T. Tolker-Nielsen, B. Koch, M. Givskov and S. Kjelleberg, *J. Bacteriol.*, 2003, **185**, 4585.
11. P. Tawakoli, A. Al-Ahmad, W. Hoth-Hannig, M. Hannig and C. Hannig, *Clin. Oral Investig.*, 2013, **17**, 841.
12. (a) J. P. Blinco, K. E. Fairfull-Smith, B. J. Morrow and S. E. Bottle, *Aust. J. Chem.*, 2011, **64**, 373; (b) M. H. Lim, D. Xu and S. J. Lippard, *Nat. Chem. Biol.*, 2006, **2**, 375; (c) M. H. Lim, B. A. Wong, W. H. Pitcock, D. Mokshagundam, M. Baik and S. J. Lippard, *J. Am. Chem. Soc.*, 2006, **128**, 14364.
13. J. P. Blinco, K. E. Fairfull-Smith, B. J. Morrow and S. E. Bottle, *Aust. J. Chem.*, 2011, **64**, 373.
14. (a) G. G. Borisenko, I. Martin, Q. Zhao, A. A. Amoscato and V. E. Kagan, *J. Am. Chem. Soc.*, 2004, **126**, 9221; (b) N. Medvedeva, V. V. Martin, A. L. Weis and G. I. Likhtenshten, *J. Photochem. Photobiol. A*, 2004, **163**, 45; (c) Y. Tang, F. He, M. Yu, S. Wang, Y. Li and D. Zhu, *Chem. Mater.*, 2006, **18**, 3605.
15. (a) N. J. Agard, J. A. Prescher and C. R. Bertozzi, *J. Am. Chem. Soc.*, 2004, **126**, 15046; (b) J. A. Codelli, J. M. Baskin, N. J. Agard and C. R. Bertozzi, *J. Am. Chem. Soc.*, 2008, **130**, 11486; (c) E. M. Sletten, G. de Almeida and C. R. Bertozzi, *Org. Lett.*, 2014, **16**, 1634.
16. F. Friscourt, C. J. Fahrni and G.-J. Boons, *J. Am. Chem. Soc.*, 2012, **134**, 18809.
17. G. O'Mahony, *Synlett*, 2004, **2004**, 572.
18. (a) V. V. Rostovtsev, L. G. Green, V. V. Fokin and K. B. Sharpless, *Angew. Chem. Int. Ed. Engl.*, 2002, **41**, 2596; (b) C. W. Tornøe, C. Christensen and M. Meldal, *J. Org. Chem.*, 2002, **67**, 3057.
19. C. Sun, W. Shi, Y. Song, W. Chen and H. Ma, *Chem. Commun.*, 2011, **47**, 8638.
20. (a) C. Khin, M. D. Lim, K. Tsuge, A. Iretskii, G. Wu and P. C. Ford, *Inorg. Chem.*, 2007, **46**, 9323; (b) L. E. McQuade, M. D. Pluth and S. J. Lippard, *Inorg. Chem.*, 2010, **49**, 8025.
21. (a) V. C. Ezeh and T. C. Harrop, *Inorg. Chem.*, 2013, **52**, 2323; (b) M. H. Lim, B. A. Wong, W. H. Pitcock, D. Mokshagundam, M.-H. Baik and S. J. Lippard, *J. Am. Chem. Soc.*, 2006, **128**, 14364; (c) L. E. McQuade and S. J. Lippard, *Inorg. Chem.*, 2010, **49**, 7464.
22. M. Lee, N. G. Gubernator, D. Sulzer and D. Sames, *J. Am. Chem. Soc.*, 2010, **132**, 8828.
23. X. Huang, Y. Dong, Q. Huang and Y. Cheng, *Tetrahedron Lett.*, 2013, **54**, 3822.
24. M. Petit, C. Tran, T. Roger, T. Gallavardin, H. Dhimane, F. Palma-Cerda, M. Blanchard-Desce, F. C. Acher, D. Ogden and P. I. Dalko, *Org. Lett.*, 2012, **14**, 6366.
25. M. D. Pluth, M. R. Chan, L. E. McQuade and S. J. Lippard, *Inorg. Chem.*, 2011, **50**, 9385.

Organic & Biomolecular Chemistry Accepted Manuscript

This journal is © The Royal Society of Chemistry 2015